
MULTIBLOCK-NETWORKS: A NEURAL NETWORK ANALOG TO COMPONENT BASED METHODS FOR MULTI-SOURCE DATA

A PREPRINT

• **Anna Jenul**

Faculty of Science and Technology
Norwegian University of Life Sciences
anna.jenul@nmbu.no

• **Stefan Schrunner**

Faculty of Science and Technology
Norwegian University of Life Sciences
stefan.schrunner@nmbu.no

• **Runar Helin**

Faculty of Science and Technology
Norwegian University of Life Sciences
runar.helin@nmbu.no

• **Kristian H. Liland**

Faculty of Science and Technology
Norwegian University of Life Sciences
kristian.liland@nmbu.no

• **Cecilia M. Futsaether**

Faculty of Science and Technology
Norwegian University of Life Sciences
cecilia.futsaether@nmbu.no

• **Oliver Tomic**

Faculty of Science and Technology
Norwegian University of Life Sciences
oliver.tomic@nmbu.no

September 22, 2021

ABSTRACT

Training predictive models on datasets from multiple sources is a common, yet challenging setup in applied machine learning. Even though model interpretation has attracted more attention in recent years, many modeling approaches still focus mainly on performance. To further improve the interpretability of machine learning models, we suggest the adoption of concepts and tools from the well-established framework of component based multiblock analysis, also known as chemometrics. Nevertheless, artificial neural networks provide greater flexibility in model architecture and thus, often deliver superior predictive performance. In this study, we propose a setup to transfer the concepts of component based statistical models, including multiblock variants of principal component regression and partial least squares regression, to neural network architectures. Thereby, we combine the flexibility of neural networks with the concepts for interpreting block relevance in multiblock methods. In two use cases we demonstrate how the concept can be implemented in practice, and compare it to both common feed-forward neural networks without blocks, as well as statistical component based multiblock methods. Our results underline that multiblock networks allow for basic model interpretation while matching the performance of ordinary feed-forward neural networks.

Keywords Multiblock model · Component based method · Artificial neural network · Multi-source data · Data fusion

1 Introduction

Numerous applied prediction tasks across disciplines involve input from more than one data source, including use cases in industry [7], biology [2] and environmental sciences [8]. Even though many models ignore such information and concatenate all sources to a common data matrix, two major aspects suggest that it is advantageous to include information on input data blocks in machine learning models: firstly, the grouping of features adds additional information to the model, which might enhance model performance. Secondly, interpretation of the trained model by the user is facilitated if parameters contributing to the output can be traced back to a specific data source. Approaches

Table 1: Approaches for multiblock methods.

	two-step training	end-to-end training
CBM	CPCA/HPCA/MFA	ROSA / SO-PLS
ANN	multiblock two-step ANN	multiblock end-to-end ANN

to target these problems are closely related to data fusion, where input from multiple sensors needs to be processed simultaneously.

Setups involving multiple data sources have been successfully tackled by multiblock methods, where each block corresponds to one data source. Multiblock methods are extensively studied in the field of chemometrics [5], typically employing component based methods (CBM). Such approaches are based on well-established statistical foundations like principal component regression (PCR) [4], which consists of two major steps: step 1 performs an unsupervised dimensionality reduction, followed by a supervised training step on the reduced dataset in step 2. PCR in particular comprises an (unsupervised) Principal Component Analysis (PCA) for dimensionality reduction and an Ordinary Least Squares regression (OLS) to map PCA output to the target. Several multiblock extensions of PCA have been developed, for instance, consensus PCA (CPCA) and hierarchical PCA (HPCA) [14], multiple factor analysis (MFA) [1] and parallel factor analysis (for equally sized blocks) (PARAFAC) [6]. We will focus on HPCA where the blocks are connected through a set of super scores for each observation and super weights for each feature which captures the joint information across blocks. After HPCA decomposition, the super scores can be input to an OLS to create an HPCR hybrid.

An alternative approach to two-step training in CBM is to pursue an end-to-end training paradigm. Representatives of this approach are mainly based on partial least squares regression (PLS) [15]: in contrast to two-step methods, the dimensionality reduction step involves the target variable and thus delivers components that are more targeted towards the specific prediction problem but can be less generalizable if the setup is changed. In multiblock data analysis, this scheme is adopted by Sequential Orthogonalized PLS (SO-PLS) [11] and Response-Oriented Sequential Alternation (ROSA) [10]. Both deploy an end-to-end training paradigm, which is an extension of the PLS method to multiblock scenarios. SO-PLS assumes that blocks are presented to the model in a predefined order, whereas ROSA avoids any block prioritization.

Even though CBMs perform well in many applications, they cannot exploit the full potential and model flexibility offered by modern artificial neural networks (ANN). In particular, their structure restricts the type of input data to vector-based inputs. On the other hand, ANNs are criticized for limited interpretability. For this reason, transferring the scheme pursued by CBM to neural network architectures, denoted as multiblock networks, promises to exploit both the flexibility and interpretability of multiblock data. We propose such networks for both two-step and end-to-end training. In a case study conducted on datasets from healthcare and spectroscopy, we benchmark the performances of the proposed neural network architectures to both multiblock CBMs from the field of chemometrics, as well as baseline models without block structure. To this end, we discuss the benefits and drawbacks of the evaluated approaches.

Parts of our work are inspired by recent work from Mishra and Passos [12], who take a similar approach to analyze multi-source data. Their presented neural network topology can be seen as a special case of the presented end-to-end training concept in this paper. Our framework goes one step further and (a) includes the option to perform two-step training using neural networks, and (b) delivers an option to quantify the contribution of each block to the model output, which is valuable for the purpose of interpretation. In particular, we deliver a possibility to quantify how much a block contributes to the final model, which carries the potential to reduce computation time and storage space, as well as to save resources for data collection.

2 Multi-block networks

We present two-step training and end-to-end training architectures of ANNs, which are inspired by the analog CBM approaches. All network types are prototypes, which can easily be adapted to more flexible input data, such as by integrating CNN layers for an image or time-dependent data. We divide the approaches discussed in this study into two groups: two-step training versus end-to-end training approaches, see Table 1.

In mathematical terms, we denote the data input by $\mathbf{x} \in D \subset \mathbb{R}^N$, $N \in \mathbb{N}$, following a probability distribution $\mathbf{x} \sim P_{\mathbf{X}}$. To account for block structure, the input space is decomposed into a direct sum of subspaces $D = \bigoplus_{i=1}^B D_i$, each corresponding to one block $i = 1, \dots, B$. The univariate target variable is denoted as $y \in T \subset \mathbb{R}$ with a

corresponding probability distribution $y \sim P_Y$. Based on training model parameters $\mathbf{w} \in W \subset \mathbb{R}^M$, the goal of the predictive model is to determine a function $f_{\mathbf{w}} : D \rightarrow T$, which most adequately maps the input to the output. Given training data (\mathbf{x}, y) , the quality of the mapping is determined by the predefined loss function $e : D \times T \rightarrow \mathbb{R}^+$, leading to an optimization problem

$$\mathbf{w}^* = \min_{\mathbf{w} \in W} e(f_{\mathbf{w}}(\mathbf{x}), y).$$

2.1 Two-step training

In unsupervised deep learning, autoencoders are major representatives of unsupervised architectures. Autoencoders are trained to reconstruct an input signal with minimal loss after compressing the data. This compression step, denoted as bottleneck, represents a low-dimensional encoding and thus, a dimensionality reduction step of a similar type as the result delivered by PCA. Therefore, *multiblock two-step training networks* (two-step ANNs) involving autoencoders will be introduced as the analog to CBM methods with separate dimensionality reduction steps.

An autoencoder $f_{\mathbf{w}}^{(\text{AE})} : D \rightarrow D$ is build from an *encoder* part $f_{\mathbf{w}^{(1)}}^{(1)} : D \rightarrow R$ and a *decoder* part $f_{\mathbf{w}^{(2)}}^{(2)} : R \rightarrow D$, such that $f_{\mathbf{w}}^{(\text{AE})} = f_{\mathbf{w}^{(2)}}^{(2)} \circ f_{\mathbf{w}^{(1)}}^{(1)}$, and $\mathbf{w} = (\mathbf{w}^{(1)}, \mathbf{w}^{(2)})$. The encoder $f_{\mathbf{w}^{(1)}}^{(1)}(\cdot)$ delivers a compressed representation of the data, but has lower dimension, $\dim(R) < \dim(D)$. In order to trigger the intended behavior, $f_{\mathbf{w}}^{(\text{AE})}$ is trained to reproduce the input data \mathbf{x} by minimizing a loss function $e(f_{\mathbf{w}}^{(\text{AE})}(\mathbf{x}), \mathbf{x})$, such that $f_{\mathbf{w}}^{(\text{AE})}(\mathbf{x}) \approx \mathbf{x}$. Thus, $f_{\mathbf{w}_1}^{(1)}$ and $f_{\mathbf{w}_2}^{(2)}$ are trained towards a mutual pseudo-inverse property, which is facilitated by designing the network architectures of $f_{\mathbf{w}_1}^{(1)}$ and $f_{\mathbf{w}_2}^{(2)}$ in a symmetric way to each other. After training, dimensionality reduction is achieved by applying the encoder $f_{\mathbf{w}_1}^{(1)}$ to input data \mathbf{x} . In case of block-wise inputs, we train one autoencoder per block, given as $f_{\mathbf{w}_i}^{(\text{AE})}$, where $\mathbf{x}_i \in D_i$ is the subvector of $\mathbf{x} \in D$ corresponding to block i and the encoded space R_i is a lower-dimensional space than D_i .

Similar to the dimensionality reduction provided by PCA, autoencoders can handle high-dimensional input data and deliver a predefined dimension of the output. However, while PCA allows the number of output dimensions to be determined after training, autoencoders require that the architecture is defined beforehand. While PCA delivers an optimal linear decomposition of the input and focuses on combining the most relevant mutual information between input features, autoencoders provide more flexibility by delivering a non-linear transformation and optimizing with respect to the importance of a feature for the reconstruction of the input.

In PCR, an OLS regression model is built on top of PCA to map the PCA output to the target variable y . In the analog case of multiblock ANNs, this model combines the information from all blocks after dimensionality reduction and will

be denoted as a *blender* $b_{\mathbf{w}} : \bigoplus_{i=1}^B R_i \rightarrow T$, where $R = \bigoplus_{i=1}^B R_i$ is a direct sum containing the encoded representations

of all blocks delivered by the autoencoders with dimension $\dim(R) = \sum_{i=1}^B \dim(R_i) < \sum_{i=1}^B \dim(D_i) = \dim(D)$. The

ANN architecture for the blender part will be a dense feed-forward network. In summary, the model function $f_{\mathbf{w}}$ is composed of block-wise encoders $f_{i, \mathbf{w}_i}^{(1)}$ and a blender network $b_{\mathbf{w}}$. Figure 1 sketches the two training steps:

1. training an autoencoder $f_{i, \mathbf{w}_i}^{(\text{AE})}$ on training samples \mathbf{x}_i for each block $i = 1, \dots, B$ (unsupervised),
2. training a single blender $b_{\mathbf{w}}$ on encoded training samples $f_{i, \mathbf{w}_i}^{(1)}(\mathbf{x}_i)$ from all blocks $i = 1, \dots, B$, and labels y .

2.2 End-to-end training

The alternative approach to uncoupled dimensionality reduction and prediction steps is to use a model unifying both steps. Such models promise to fit the problem setup more accurately since information on the target variable can be exploited already in the dimensionality reduction step. The component based reference models SO-PLS and ROSA pursue an iterative scheme, where blocks are orthogonalized with respect to those blocks already processed.

A direct equivalent to the scheme of ROSA and SO-PLS is presented by *multiblock end-to-end training networks* (end-to-end ANN). The block-wise input is presented to distinct branches of the network, where each branch involves a sub-network that processes the block over multiple layers and may be of a similar type as the encoder part of the autoencoder. However, instead of training each branch separately, the one- or multi-dimensional output of each branch is connected to the blender network $b_{\mathbf{w}}$, such that the network $f_{\mathbf{w}}$ directly maps the block input to the target variable.

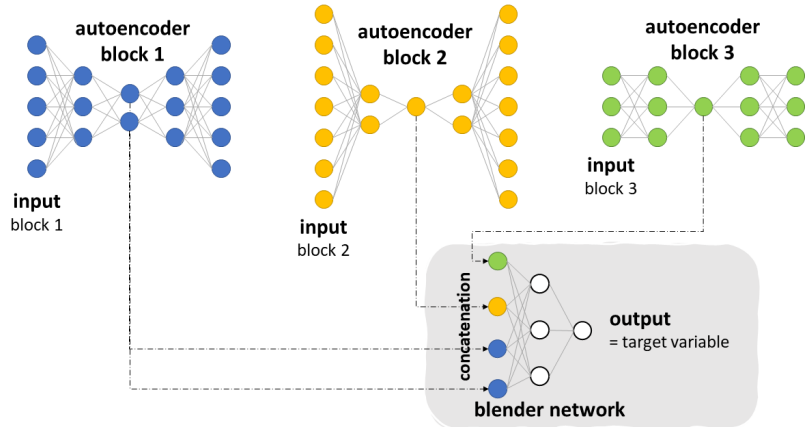


Figure 1: Multiblock two-step ANN architecture.

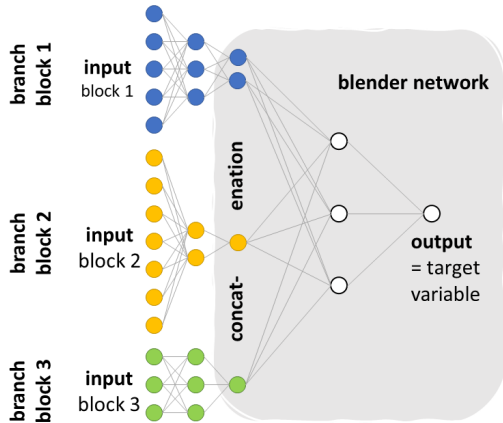


Figure 2: Multiblock end-to-end ANN architecture.

The training procedure is conducted in a single step, where data from all blocks are processed through the network and errors are computed for the predicted output $f_w(x)$ and the actual target value y . The architecture of a multiblock end-to-end ANN is illustrated in Figure 2.

2.3 Quantifying block relevance

A major motivation for deploying multiblock methods is the assessment of the predictive power of each block on the target variable. CBM approaches deliver a profound statistical framework, which allows analysis of block importance via (a) the number of selected components from each block, and (b) the ratio of explained variance from each block. In the multiblock network setup, the corresponding concept to selecting a number of components from each block is to define the number of nodes of the block branches before entering the concatenation layer of the blender network. The block nodes must be specified by the user in advance. Thus, quantification of block relevance requires an alternative approach.

ANNs use two conjugate sources of information that can potentially be exploited to quantify block relevance: (1) trained model weights, including the weights between nodes and the bias added to each layer, and (2) activations. Model weights remain static after completing the training phase, while activations are the pieces of information passed over the network. For this purpose, it is essential to investigate the blender part b_w of the network, where the block information is mapped to the final target variable.

Node activations represent the units of information passing through the ANN. In the concatenation layer illustrated in Figures 1 and 2, where information from the blocks enters the blender network, the activation is of particular importance since it encodes the block information. We denote the concatenation layer nodes by c_i , where the index i represents the blocks $i = 1, \dots, N$. When model input \mathbf{x} is passed through the network, the activation of node c_i , denoted as $c_i(\mathbf{x})$, is obtained. After training all network weights, we quantify the relevance of a block for the final output, by evaluating the pseudo-output, which is delivered if we pass the input of only one block at a time through the network: assuming that only one node is associated with each block in the concatenation layer, we input the vector

$$v_i = \begin{cases} c_j(\mathbf{x}) & \text{if } j = i \\ 0 & \text{otherwise,} \end{cases}$$

$i = 1, \dots, N$, into the blender network b_w and obtain the pseudo-output $b_w(v_i)$. In case that a block i has multiple associated nodes in the concatenation layer $c_i^{(1)}, \dots, c_i^{(n)}$, we generalize v_j to

$$v_j = \begin{cases} c_j(\mathbf{x}) & \text{if } c_j \in \{c_i^{(1)}, \dots, c_i^{(n)}\} \\ 0 & \text{otherwise.} \end{cases}$$

In addition, we compute the output of the neural network involving the full information from all blocks, which is described by $f_w(\mathbf{x})$. We assume that blocks with relevant impact on the final result deliver a more similar pseudo-output $b_w(v_i)$ and output $f_w(\mathbf{x})$ than those which contribute less to the result.

Across all training samples, we propose the following measure for block relevance: if h_{f_w} denotes the histogram of model outputs and $h_{b_w,i}$ denotes the histogram of pseudo-outputs with respect to block i , block relevance is measured by the Jensen-Shannon (JS) divergence $D_{JS}(h_{b_w,i}, h_{f_w})$, representing a dissimilarity measure between h_{f_w} and $h_{b_w,i}$. The JS divergence is a similarity measure for two probability distributions p and q with equal supports $S = \{\mathbf{x} : p(\mathbf{x}) \neq 0\} = \{\mathbf{x} : q(\mathbf{x}) \neq 0\}$, based on the Kullback-Leibler divergence D_{KL} . For discrete probability distributions, the JS divergence is defined as

$$D_{JS}(p, q) = \frac{1}{2} (D_{KL}(p, m) + D_{KL}(q, m)),$$

where $m(\mathbf{x}) = \frac{1}{2} (p(\mathbf{x}) + q(\mathbf{x}))$ and

$$D_{KL}(p, q) = \sum_{\mathbf{x} \in S} p(\mathbf{x}) \log \left(\frac{p(\mathbf{x})}{q(\mathbf{x})} \right).$$

The JS divergence delivers a value between 0 and 1, where a low value indicates a strong similarity between the distributions, such that the full output h_{f_w} is to a large extent explained by the pseudo-output $h_{b_w,i}$ of the corresponding block. A high JS divergence indicates that the corresponding block does not contribute significantly to the model output. Even though the absolute range of the JS divergence value might not be informative due to different shapes of the probability distributions, the relative ranking among the blocks reveals their impact on the model output. In an example with 3 blocks, the scheme of comparing the pseudo-outputs to the full output is illustrated in Figure 3.

3 Experiments & Results

We evaluate two use cases, one with a binary target and one with a continuous target, where the presented multiblock network architectures are compared to CBM approaches ROSA and HPCR, as well as to baseline models.¹

3.1 Use Case 1: Breast Cancer Wisconsin dataset

The Breast Cancer Wisconsin dataset (BCW) [13] describes a binary classification problem (malignant or benign tumour) and consists of 212 malignant and 357 benign samples. Features are based on 10 continuous characteristics extracted from medical image data, including the "perimeter" and "texture" of cell nuclei on an image from a fine needle aspirate. For each of the 10 characteristics, the *mean*, *standard deviation* and *worst values* are measured across all cell nuclei on the image, resulting in three blocks with 10 features each. Hence, for the characteristic "perimeter", block 1 (MN) contains feature "mean perimeter", block 2 (STD), "standard deviation perimeter" and block 3 (WO) "worst perimeter". Across the three blocks, particularly features corresponding to the same characteristics in MN and WO are highly correlated. Related research on the dataset showed that WO carries the highest information about the target variable, followed by MN and STD with the lowest information [9].

¹[https://archive.ics.uci.edu/ml/datasets/Breast+Cancer+Wisconsin+\(Diagnostic\)](https://archive.ics.uci.edu/ml/datasets/Breast+Cancer+Wisconsin+(Diagnostic)) and <https://data.mendeley.com/datasets/46htwnp833/2>.

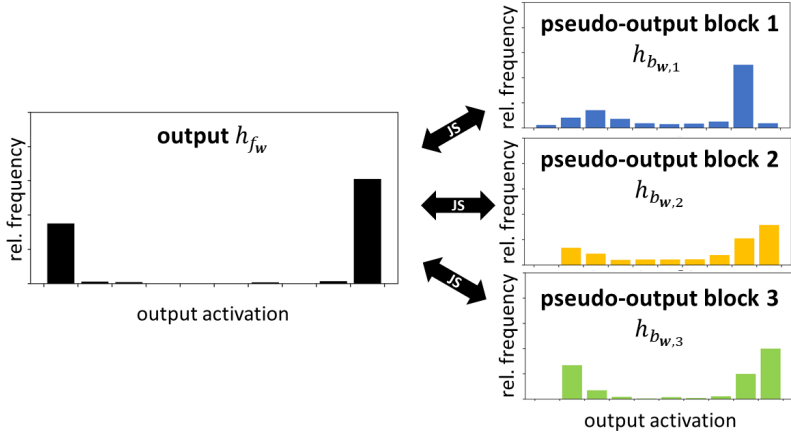


Figure 3: To quantify block relevance for the model, pseudo-outputs corresponding to each block are compared to the full model output, which includes all blocks simultaneously.

We split the dataset into a stratified train (75%) and test (25%) set and standardize both sets feature-wise using the mean and the standard deviation of the train set. The results for both the ANN and the CBM are evaluated with the metrics F_1 -score (f1), precision (pr), recall (rc), accuracy (acc) and Matthew’s correlation coefficient (mcc).

The multiblock networks (both, two-step and end-to-end approaches) consist of a functional network structure where each block is modelled with an identical architecture. It is possible to further adapt the architecture for each block, but the given setup is intended as a proof of concept of the multiblock architecture. Each block branch consisting of a sequence of the input layer and four dense layers with 10, 10, 3 and 1 nodes, respectively, and elu activation functions, similar to Figure 2. Before the three blocks are merged in the concatenation layer, we deploy batch normalization to transform the blocks to a common scale. The blender part of the network starts with a concatenation layer, passes the information over two dense layers with three nodes and elu activations each, and ends with the final output layer containing a single node (sigmoid activation). In order to train the network, we use the adam optimizer and a batch size of 100. After determining the number of epochs using 5-fold cross-validation (80 epochs for end-to-end and 750/1200 epochs for training the autoencoder/blender of the two-step network are optimal), we train the described multiblock network 50 times with independent weight initializations to reduce the influence of randomness — all metrics are averaged over these 50 runs. The runtimes² for a single run of each method are presented in Table 2. For the two-step ANN, the computation is significantly slower compared to the other approaches, because an independent autoencoder is trained for each block before the blender network. Furthermore, higher numbers of epochs are required to reach comparable performances.

In contrast to the multiblock networks, CBMs provide deterministic results since they do not rely on random weight initialization. We select a number of 5 components for the ROSA and HPCR model, respectively. A logistic regression model (LR) serves as the baseline on the dataset. Results are shown in Table 2.

Even though the performance is very high across all approaches and metrics, end-to-end approaches outperform two-step approaches, since they make use of the target variable during training of all model parts. The multiblock network matches the performance of the fully connected network, with the major benefit of being able to interpret single block contributions. Figure 4(a) illustrates the distributions of the JS divergence over the 50 independent runs for the three blocks. Most of the JS values for the WO block accumulate close to 0, indicating that a large proportion of the 50 models deliver an output very close to the real output. This is a strong indication that WO is an important block for prediction. In contrast, the median in the "mini-bloplot" inside the violin is considerably higher for STD, indicating that it is of lesser importance. Similarly to WO, JS values for MN are close to zero but with a higher proportion distributed over the entire interval 0-1. This result is not surprising, as MN and WO are highly correlated, leading to balanced models where each of the 50 models chooses either of these two blocks to perform well. In conclusion, the end-to-end approach states that WO is the most relevant block, MN is slightly less important and STD contributes little to the output.

²Ubuntu Linux v20.04.1 LTS, Intel Core i5-8265U CPU @ 1.60GHz, 16 GB RAM, Python 3.8.10, TensorFlow v2.5.0, R Studio v1.4.1106, R v4.1.0

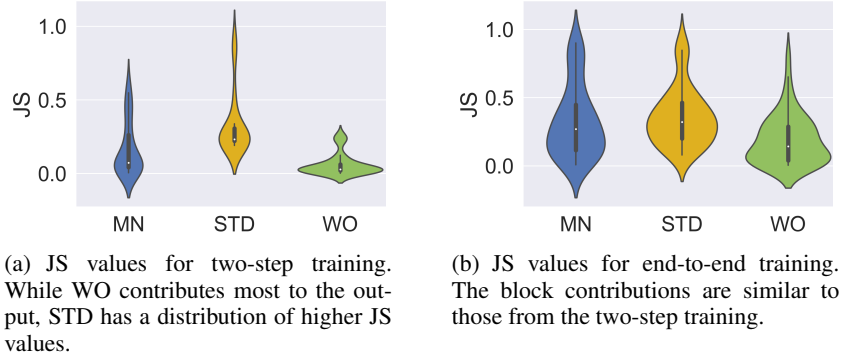


Figure 4: Distributions of JS divergence for the three blocks. For both multiblock ANN approaches, WO has the distribution closest to zero.

Table 2: Performance of prediction methods on the BCW dataset. For ANN setups, mean values are provided across model runs. All standard deviations are below 0.02. The runtime [s] is computed for a single run.

metric	baseline		multiblock ANN		multiblock CBM	
	ANN	LR	two-step	end-to-end	HPCR	ROSA
f1	0.97	0.90	0.94	0.97	0.90	0.93
pr	0.97	0.89	0.93	0.96	0.96	0.98
rc	0.97	0.91	0.96	0.97	0.85	0.89
acc	0.96	0.92	0.93	0.96	0.93	0.95
mcc	0.91	0.84	0.85	0.91	0.85	0.90
runtime	1.7	≤0.1	37.9	3.0	≤0.1	≤0.1

The block contributions evaluated from multiblock ANN approaches are more accentuated for the two-step approach than for the end-to-end training, as shown in Figure 1. WO has the lowest JS values, followed by MN and STD. Table 3 presents the mean and standard deviation of the JS values for each block. In addition, we indicate how often each block had the lowest JS value over the 50 models.

On the other hand, the component based methods perform equally well to the ANNs on the BCW dataset. Similarly to the ANN models, the supervised ROSA outperforms unsupervised HPCR. Analyzing the deterministic ROSA results, Figure 5 gives an overview of how the extracted components of each block contribute to explain the variance of the target variable. The color gradient from dark blue to dark red indicates when a component was added to the ROSA model. In this example, the first component is selected from WO and explains already approximately 70% of the variance in the target variable. Hence, WO contributes most of the predictive performance and is the most important block of the BCW dataset. Three of the remaining four components are selected from the other two blocks (2 from MN and 1 from STD) but add only little information to the model. Overall the results from ROSA match well with the block contributions acquired by the multiblock networks.

Table 3: Distribution of JS values (mean ± standard deviation) for each block after multiblock ANN training, as well as the number of model runs (out of 50), where the pseudo-output from a block is most similar to the full output model, i.e. has the lowest JS value (# lowest). 0.00* indicates a value between 0 and 0.005.

dataset	block	two-step ANN		end-to-end ANN	
		JS	# lowest	JS	# lowest
BCW	MN	0.17 ± 0.18	10	0.33 ± 0.26	17
	STD	0.33 ± 0.21	0	0.36 ± 0.21	5
	WO	0.06 ± 0.07	40	0.19 ± 0.18	28
mango	Vis	0.02 ± 0.01	1	0.30 ± 0.02	0
	NIR	0.00 ± 0.01	49	0.00 ± 0.00*	50

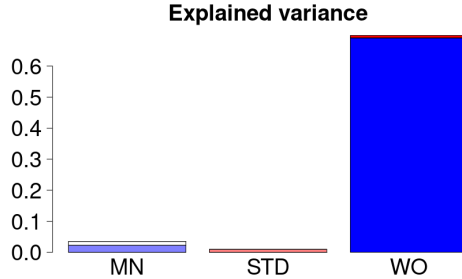


Figure 5: The stacked histogram shows how much single components contribute to the explained variance of the target in the ROSA model. While one component from WO explains approximately 70%, the components extracted from MN and STD provide only little additional information.

3.2 Use Case 2: Mango dataset

The mango dataset [3] consists of spectra in the visible (Vis) near-infrared (NIR) range taken from mango fruits. The spectra are used to predict the amount of dry matter (DM) in the samples. Each spectrum spans the wavelength range 350 - 1200 nm with 3 nm spacing. For this analysis, the data was divided into a Vis-block (450 - 696 nm) and a NIR-block (699 - 1029 nm) where the endpoints were removed due to noise. The owners of the dataset have divided the data into a train set of 10 243 fruit samples harvested between 2015 and 2017 and a test set of 1 448 samples harvested in 2018. We deploy the preprocessing scheme and network architecture suggested by Mishra and Passos [12] with minor modifications: prior to the analysis the train set was subjected to outlier removal via Hotelling’s T^2 and Q statistics based on PLS decomposition. After outlier removal, the final train set contained 9 926 samples.

Each block of the mango dataset is modelled by three fully connected layers with 36, 18 and 12 nodes, respectively, in the two-step approach. The optimal filter sizes of the convolutional layers were 21 for the Vis block and 13 for the NIR block, found by using 3-fold cross-validation on the training data. The blender part of the network consists of two fully connected layers with 4 and 1 nodes, respectively, after the output of the two single-block networks had been concatenated. The outputs of the block networks use sigmoid activation, the final layer of the blender part uses linear activation and the rest of the network uses elu activation. All the model weights were subject to L2-regularization with a strength of 0.01. The architecture for the end-to-end network is mainly identical to the two-step approach, but additionally includes a 1D convolutional layer for each block (using stride equal to 1 and without adding zero-padding before the convolution).

For the CBM approaches, we use the well-established preprocessing Standard Normal Variates (centering and scaling the blocks row-wise), in addition to the outlier. No further data transformation techniques are applied. Similar to the BCW dataset we decide on 10 components for ROSA — the same number of components is used for HPCR, as well. We determine the root mean squared error (RMSE) and the R^2 -score (R^2) on the test set, see Table 4. For the baseline linear regression model (LM) we scale row-wise across both blocks.

Table 4 shows that the end-to-end multiblock ANN outperforms the baseline linear model and the CBMs. However, an advantage of CBM methods is their significantly faster computation time. Two-step techniques, HPCR and multiblock two-step ANNs provide much poorer performance since the essential information content for predicting the target variable cannot be extracted accurately from the dataset. Even though the fully connected ANN delivers predictions with similar performance as the multiblock end-to-end approach, the latter is able to quantify the block contributions precisely, see Figure 6. The JS divergence of the NIR block is very close to 0, whereas the JS divergence for Vis is significantly higher, suggesting that most information is provided by the NIR block. A similar conclusion can be drawn from the ROSA model, where the percentage of explained variance of the target reaches more than 80% with one component from the NIR block, see Figure 7. Even though several components were extracted from Vis it contributes little to the explained variance of the target. Summarizing the results, the multiblock ANNs agree with ROSA on the fact that most information is stored in the NIR block.

4 Discussion

Both multiblock ANN and CBM approaches are able to match or exceed the predictive performances of baseline models. Moreover, they provide the additional advantage of linking the prediction back to single blocks. Potential

Table 4: Performance of prediction methods on the mango dataset. For ANN setups, mean values across all runs are provided, the standard deviation is below 0.07 in all cases. The runtime [s] is measured for a single run.

metric	baseline		multiblock ANN		multiblock CBM	
	ANN	LM	two-step	end-to-end	HPCR	ROSA
RMSE	0.91	1.08	2.78	0.94	2.56	1.00
R ²	0.89	0.84	-0.09	0.88	0.08	0.86
runtime	274.4	0.36	160.2	398.4	47.9	1.5

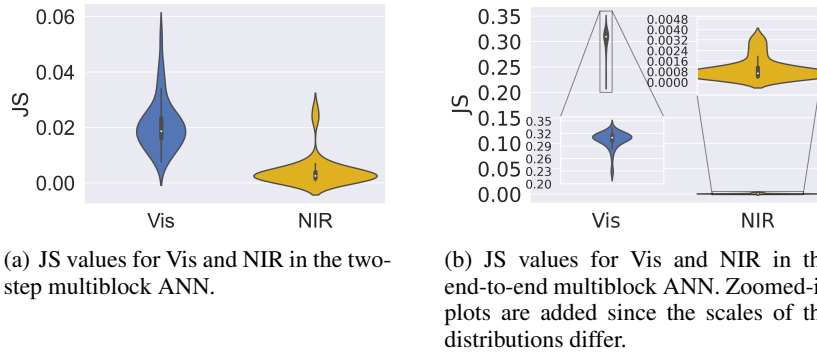


Figure 6: Distributions of JS values between pseudo-outputs for each block and the full output, respectively, involving inputs from all blocks simultaneously. For the two-step approach, both blocks deliver JS values close to 0, whereas for the end-to-end training Vis yields much higher values than NIR.

savings can be achieved by not collecting data from sources with minor relevance for the final model, resulting in lower computational costs and storage space requirements.

In comparison to CBM approaches, the flexibility of multiblock ANNs can lead to higher predictive performance on the test dataset, given that a sufficient amount of training data is available and that the underlying information may not be linearly separable. Use case 2 demonstrates that the ability to integrate specific processing steps like convolutions directly into the trained model is a strong benefit of ANN architectures, while CBMs require more extensive preprocessing of the data before being fed to the model. To potentially improve the performance of CBMs to the level of ANNs, more effort has to be invested in preprocessing and data engineering. However, in this case, the CBM models’ advantages in model interpretation persist. Still, as illustrated in use case 1, CBM methods are able to keep up with the performance of ANNs in scenarios with smaller datasets. Regarding interpretability, multiblock ANNs offer a possibility for quantifying the contribution of each block to the network, which is a benefit over classical ANN approaches. Nonetheless, CBM models provide even deeper insights into the structure of the data, such as scores and loadings, which are beyond the scope of this study. Another aspect to consider is that most CBMs are deterministic, while ANNs depend on the weight initialization and thus, deliver slightly different models in multiple runs. From the

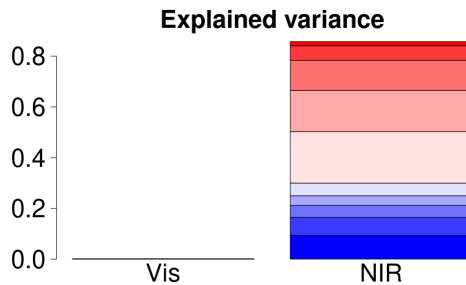


Figure 7: NIR explains more than 80% of the variation in the target variable, whereas Vis does not contribute.

perspective of computational effort, CBMs are in a lower range than ANNs, especially for smaller datasets — however, the runtime of CBMs depends heavily on the type of internal validation and preprocessing creates additional overhead.

Both two-step and end-to-end training models are able to extract relevant information from the data with respect to the target variable. Nevertheless, the end-to-end training paradigm enables the model to extract information targeted towards the output variable in all model parts, resulting in better adaption to the specific problem. In practice, this aspect leads to higher performance scores. Especially use case 2 demonstrated that separate dimensionality reduction can significantly decrease the predictive performance. Observations from additional experiments suggest that a larger number of nodes in the encoding layer, representing a weaker compression in the dimensionality reduction step, can improve the results of the autoencoder-based models. Moreover, the more general dimensionality reduction performed by two-step training models may be re-used for other problem setups, for example, if the target variable is changed. In such cases, the end-to-end model must be re-trained.

5 Conclusion

We presented a class of ANN architectures, which combine the benefits of both feed-forward neural networks and multiblock CBMs. The goal is to model datasets with multi-source input such that high predictive performance and model interpretability is maintained. The framework delivers a flexible and powerful tool, which allows the user to understand how much a block contributes to the model output. In two use cases, we analyzed the benefits and drawbacks of multiblock ANNs and CBMs, concluding that multiblock ANNs deliver a balanced trade-off between the strengths of both approaches. Thus, the presented framework is a significant extension of state-of-the-art neural network architectures and may serve as a platform for further development of interpretational tools.

References

- [1] H. Abdi, L. J. Williams, and D. Valentin. Multiple factor analysis: principal component analysis for multitable and multiblock data sets. *WIREs Computational Statistics*, 5(2):149–179, 2013.
- [2] L. M. Alnemer, O. Al-Azzam, C. Chitraranjan, A. M. Denton, F. M. Bassi, M. J. Iqbal, and S. F. Kianian. Multiple Sources Classification of Gene Position on Chromosomes Using Statistical Significance of Individual Classification Results. In *2011 10th International Conference on Machine Learning and Applications and Workshops*, volume 1, pages 7–12, 2011.
- [3] N. Anderson, K. Walsh, P. Subedi, and C. Hayes. Achieving robustness across season, location and cultivar for a NIRS model for intact mango fruit dry matter content. *Postharvest Biology and Technology*, 168:111202, 2020.
- [4] E. Bair, T. Hastie, D. Paul, and R. Tibshirani. Prediction by Supervised Principal Components. *Journal of the American Statistical Association*, 101(473):119–137, 2006.
- [5] R. G. Brereton. *Chemometrics for Pattern Recognition*. John Wiley & Sons, Ltd, 2009.
- [6] R. Bro. PARAFAC. Tutorial and applications. *Chemometrics and Intelligent Laboratory Systems*, 38(2):149–171, 1997.
- [7] P. Dagnely, T. Tourwé, and E. Tsiporkova. Annotating the Performance of Industrial Assets via Relevancy Estimation of Event Logs. In *2018 17th IEEE International Conference on Machine Learning and Applications (ICMLA)*, pages 1261–1268, 2018.
- [8] F. Farahnakian, M.-H. Haghbayan, J. Poikonen, M. Laurinen, P. Nevalainen, and J. Heikkonen. Object Detection Based on Multi-sensor Proposal Fusion in Maritime Environment. In *2018 17th IEEE International Conference on Machine Learning and Applications (ICMLA)*, pages 971–976, 2018.
- [9] A. Jenul, S. Schrunner, K. H. Liland, U. G. Indahl, C. M. Futsaether, and O. Tomic. RENT – Repeated Elastic Net Technique for Feature Selection, 2021.
- [10] K. H. Liland, T. Næs, and U. G. Indahl. ROSA—a fast extension of partial least squares regression for multiblock data analysis. *Journal of Chemometrics*, 30(11):651–662, 2016.
- [11] T. Næs, O. Tomic, B.-H. Mevik, and H. Martens. Path modeling by sequential PLS regression. *Journal of Chemometrics*, 25:28–40, 01 2011.
- [12] Puneet Mishra and D. Passos. Deep multiblock predictive modelling using parallel input convolutional neural networks. *Analytica Chimica Acta*, 1163:338520, 2021.
- [13] W. N. Street, W. H. Wolberg, and O. L. Mangasarian. Nuclear feature extraction for breast tumor diagnosis. In R. S. Acharya and D. B. Goldgof, editors, *Biomedical Image Processing and Biomedical Visualization*, volume 1905, pages 861 – 870. International Society for Optics and Photonics, SPIE, 1993.

-
- [14] J. A. Westerhuis, T. Kourti, and J. F. MacGregor. Analysis of multiblock and hierarchical PCA and PLS models. *Journal of Chemometrics*, 12(5):301–321, 1998.
- [15] S. Wold, H. Martens, and H. Wold. The multivariate calibration problem in chemistry solved by the PLS method. In B. Kågström and A. Ruhe, editors, *Matrix Pencils*, pages 286–293, Berlin, Heidelberg, 1983. Springer Berlin Heidelberg.